Preprint Title	Ferrocenophanes with two nitrogen atoms in bridging positions *via* olefin metathesis: synthesis, structure, and solution dynamics
Authors	Karol Rawiak, Maria Mazur, Tsenguun Enkhbold, Michał Sitek, Stanisław Kulczyk, Piotr Paluch, Piotr A. Guńka, Mariola Koszytkowska-Stawińska and Włodzimierz Buchowicz
Publication Date	26 Juli 2023
Article Type	Full Research Paper
Supporting Information File 1	N_ferrocenofany_1B2_SI.docx; 3.0 MB
Supporting Information File 2	pg159smart.cif; 772.7 KB
Supporting Information File 3	pg172.cif; 890.1 KB
Supporting Information File 4	pg181.cif; 2.4 MB
Supporting Information File 5	pg189.cif; 2.6 MB
Supporting Information File 6	pg190smart_sqP.cif; 6.5 MB

ORCID® iDs Maria Mazur - https://orcid.org/0000-0003-0452-1594; Stanisław Kulczyk - https://orcid.org/0000-0002-2789-1814; Piotr A. Guńka - https://orcid.org/0000-0002-0977-5246; Mariola Koszytkowska-Stawińska - https://orcid.org/0000-0002-7545-5937; Włodzimierz Buchowicz - https://orcid.org/0000-0002-1832-7461

Ferrocenophanes with two nitrogen atoms in bridging positions *via* olefin metathesis: synthesis, structure, and solution dynamics

Karol Rawiak[1], Maria Mazur[1,2], Tsenguun Enkhbold[1], Michał Sitek[1], Stanisław Kulczyk[1], Piotr Paluch[3], Piotr A. Guńka[1], Mariola Koszytkowska-Stawińska[1], Włodzimierz Buchowicz*[1]

Address:

[1] Faculty of Chemistry, Warsaw University of Technology, Noakowskiego 3, 00-664 Warsaw, Poland

[2] Łukasiewicz – Industrial Chemistry Institute, Rydygiera 8, 01-793 Warsaw, Poland

[3] Polish Academy of Sciences, Centre of Molecular and Macromolecular Studies, Sienkiewicza 112, 90-363 Łódź, Poland

Email:

Włodzimierz Buchowicz – wlodzimierz.buchowicz@pw.edu.pl

* Corresponding author

Abstract

The ruthenium-catalysed ring-closing metathesis of 1,1'-ferrocenylmethylamines provided [8]ferrocenophanes with two nitrogen atoms in the bridge and the (*E*)-configuration of the newly formed carbon-carbon double bond. The single-crystal diffraction analyses reveal that these compounds are axially chiral, while the distance between the two nitrogen atoms suggests their potential applications as bidentate ligands. The diaza[8]ferrocenophanes display intriguing solution dynamics that was investigated by means of variable temperature NMR spectroscopy. According to

theoretical calculations, the most stable conformer of the ferrocenophane in solution has both *N*-substituents occupying the pseudoequatorial positions of the macrocycle.

Keywords

ferrocene; Grubbs' catalyst; olefin metathesis; single crystal X-ray structure; variable temperature NMR

Introduction

Olefin metathesis has been successfully used in the synthesis of ferrocenophanes (*ansa*-ferrocenes) for twenty years [1, 2]. The reactions of 1,1'-diallylferrocenes (Scheme 1a) with Grubbs' catalysts [Ru(=CHPh)Cl_2(PCy_3)$_2$] (**GI**) resulted in all-carbon bridged [4]ferrocenophanes with (*Z*)-configuration of the newly formed carbon-carbon double bond [3, 4]. More recently, 1,1'-bis(but-3-enyl)ferrocenes (Scheme 1b), in the presence of catalyst **GI** or [Ru(=CHPh)Cl_2(PCy_3)(SIMes)] (**GII**), yielded [6]ferrocenophanes with geometry of the bridge depending on the type of substituents in the alkenyl chains [5].

Under similar conditions, 1,1',3,3'-tetrakis(but-3-enyl)metallocenes provided axially chiral *diansa*-metallocenes [6], while decaallylferrocene underwent a combination of inter- and intraligand ring-closing reactions [7]. Moreover, application of chiral molybdenum catalysts resulted in kinetic resolution of the planar-chiral 1,2-diallylferrocenes (Scheme 1c) [8]. Ring-closing metathesis (RCM) was also accomplished in titanocene and zirconocene dichlorides [4, 9, 10]. A noticeable example of a medicinal potential of all-carbon bridged, metathesis-derived

ferrocenophane was demonstrated in our recent report describing a [4]ferrocenophane-triazole-uracil conjugate displaying anticancer activity [11].

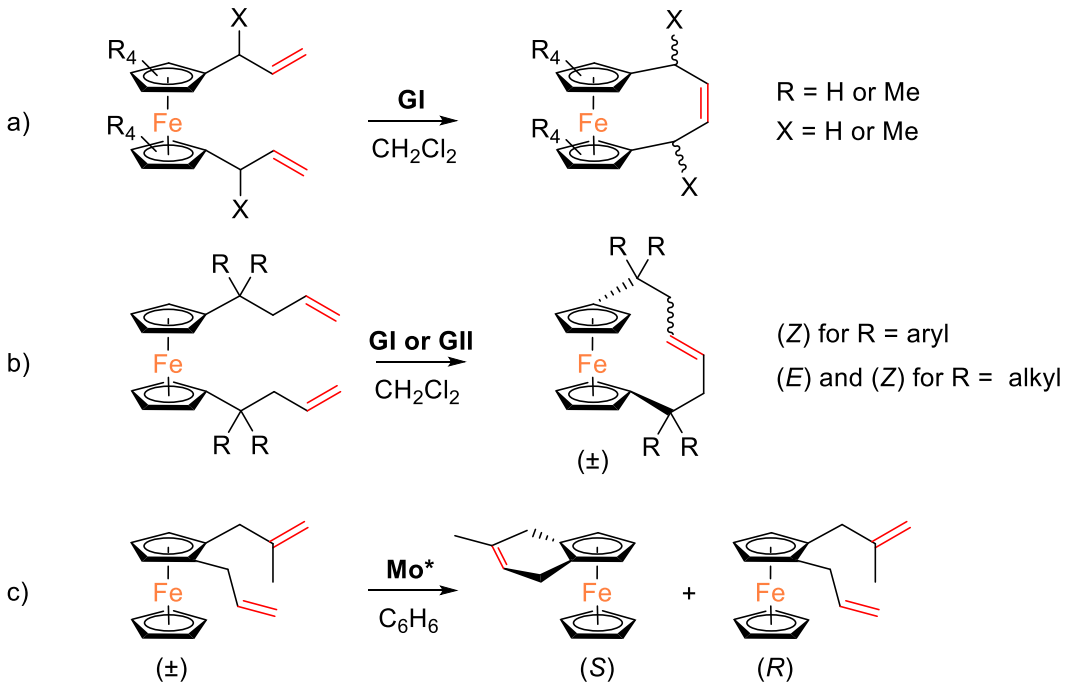

Scheme 1: (a) The ruthenium-catalysed interligand reactions of 1,1'-diallylferrocenes. (b) The ruthenium-catalysed interligand reactions of 1,1'-bis(but-3-enyl)ferrocenes. (c) The asymmetric molybdenum-catalysed intraligand resolution of 1,2-diallylferrocenes. **GI** = [Ru(=CHPh)Cl_2(PCy_3)$_2$], **GII** = [Ru(=CHPh)Cl_2(PCy_3)(SIMes)], **Mo*** = (pyrrolyl)$_2$Mo(=$CHCMe_2Ph$)(=N-C_6H_3-2,6-*i*Pr_2)/chiral biphenol.

Olefin metathesis of heteroatom-substituted ferrocenes has been studied mainly for phosphaferrocenes using molybdenum-based catalysts, including enantioselective synthesis of planar-chiral derivatives [12-15]. In a report describing preparation of ferrocene-containing polymers, a number of variously substituted allyl or homoallyl ferrocene diethers and diesters have been reacted with catalyst **GII** to yield cyclic olefins [16].

Unlike all-carbon bridged ferrocenophanes, ferrocenophanes with heteroatoms in the bridge display promising properties, such as anion sensing [17] or antitumor activity [18]. Therefore, we sought to develop a general, metathesis-based approach to diazaferrocenophanes that would tolerate a variety of functional groups. Azaferrocenophanes have been prepared thus far by different routes, usually involving multistep preparation of 1,1'-disubstituted precursors followed by their cyclization [19-25], or from bis(aminocyclopentadiene) and $FeCl_2$ [26]. We are aware of only few examples of RCM in nitrogen-functionalized ferrocenes, that is intraligand reactions in the synthesis of ferroceno-quinoline [27] or ferrocene-fused 4-pyridones [28], and an interligand one in *N*-butenyl *β*-lactams [29]. This might be attributed to the fact that amines are well-known to have detrimental effect on the efficiency of the ruthenium-catalysed olefin metathesis [30-34]. Herein, we report a straightforward synthesis and characterization of ferrocenophanes with two nitrogen atoms in bridging positions using the ring-closing metathesis reactions of suitably designed ferrocenylmethylamines.

Results and Discussion

Synthesis

The amino diene substrates for RCM reactions (Scheme 2a), that is **1a**, **1b**, **1d**, **1e**, and **1f** were synthesized by reductive amination of 1,1′-ferrocenedicarboxaldehyde with the appropiate amines and $NaBH(OAc)_3$ in 1,2-dichloroethane (DCE). The diamines with two different *N*-substituents, **1c** and **1g** (Scheme 2b), were obtained from *N*-allyl-4-methoxyaniline or *N*-allylmethylamine, respectively, and the amino

aldehyde **S1** previously prepared from the mono amination of 1,1′-ferrocene-dicarboxaldehyde with *N*-allylaniline [35].

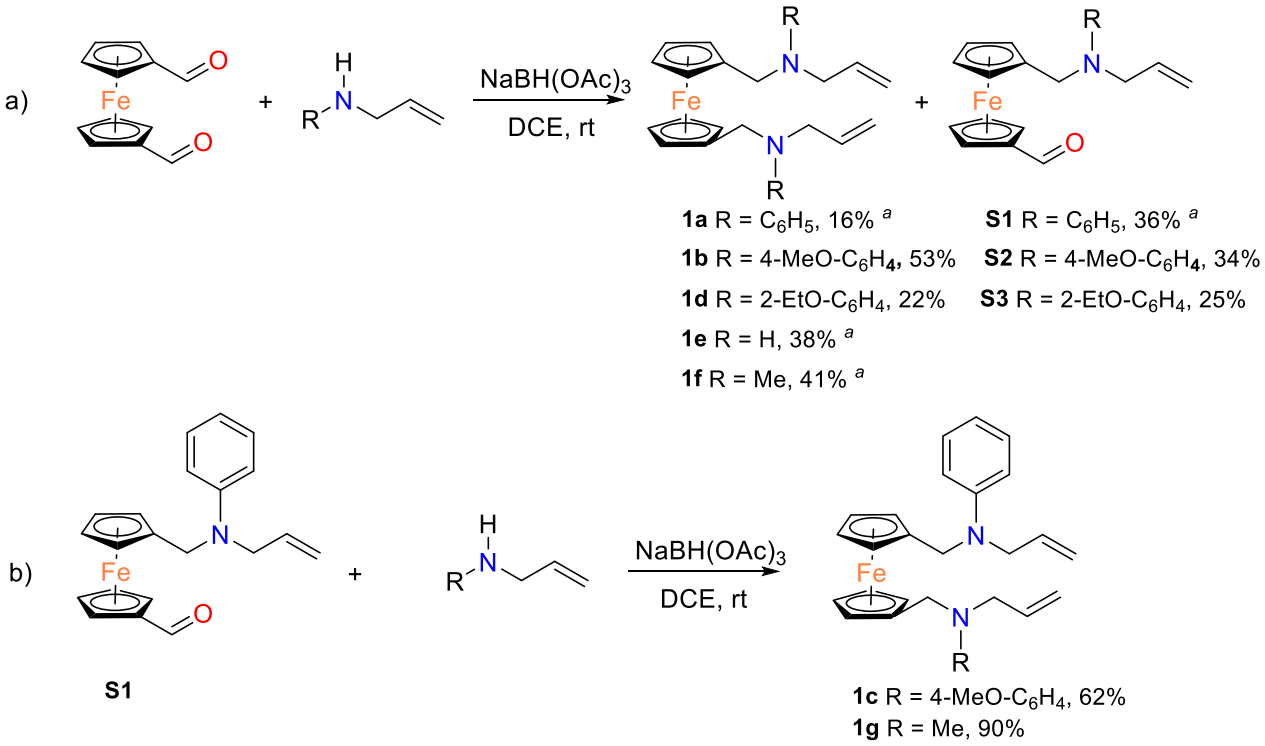

Scheme 2: Synthesis of 1,1'-bis(aminomethyl)ferrocenes **1**. Isolated yields are given; [a] data from ref. [35]. Conditions: (a) aldehyde (1 eq), amine (3-3.5 eq), $NaBH(OAc)_3$ (2.5-3.5 eq), 1,2-dichloroethane (DCE), room temperature, 1-7 days. (b) amino aldehyde **S1** (1 eq), amine (1-2 eq), $NaBH(OAc)_3$ (1 eq), DCE, room temperature, 1 day.

Reactions of aromatic diamines **1a**-**1c** with catalyst **GII** in refluxing CH_2Cl_2 provided the expected 11-membered macrocycles **2a**-**2c** (Scheme 3). Examination of the ^1H NMR spectra of crude reaction mixtures indicates that only one stereoisomer of the carbon-carbon double bond was formed in significant amounts (Figure S1). On the other hand, the RCM reactions of sterically congested substrate **1d** bearing the 2-ethoxy substituent were incomplete after several days (Scheme 3).

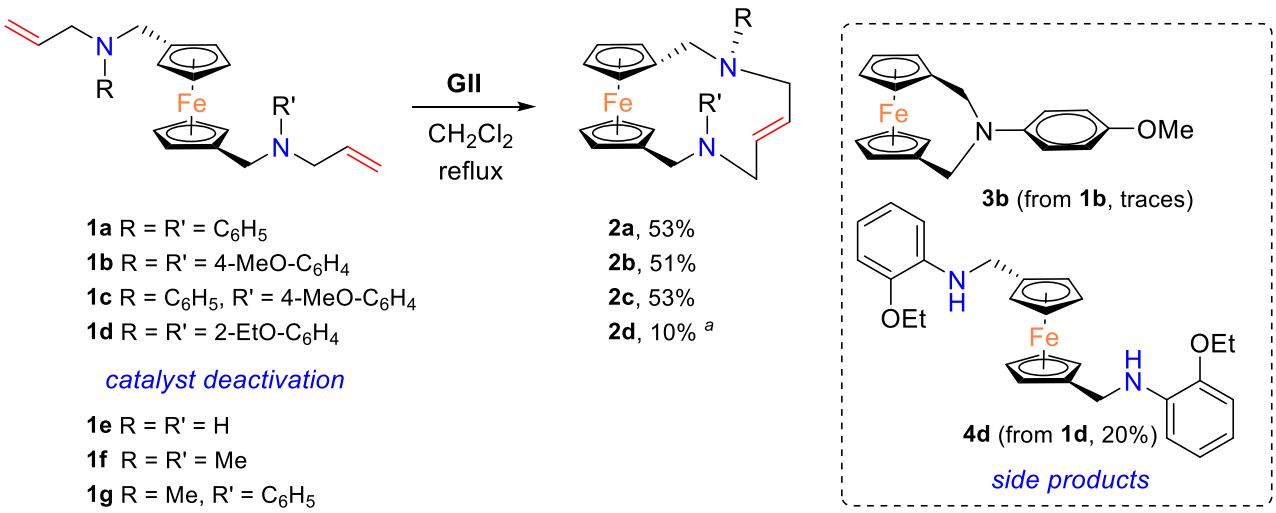

Scheme 3: The ruthenium-catalysed olefin metathesis of 1,1'-bis(aminomethyl)-ferrocenes **1**. Isolated yields are given; [a] conversion of **1d** to **2d** estimated by ^{1}H NMR after 2 weeks. Diamines **1e**, **1f**, and **1g** did not yield metathesis products. Conditions: [Ru(=CHPh)Cl$_2$(PCy$_3$)(SIMes)] (**GII**), 5-10 mol%, reflux, 5 h, then overnight at room temperature.

Surprisingly, a trace amount of *N*-aryl-2-aza[3]ferrocenophane **3b** was also isolated from the reaction of **1b** with catalyst **GII**. Since deprotection of a variety of allylic amines in the presence of **GII** in refluxing toluene has been described [36], formation of **3b** could be rationalized by deallylation of **1b** with the ruthenium species derived from **GII** and subsequent intramolecular nucleophilic substitution. *N*-Deallylation was also observed in the case of **1d**, resulting in the formation of the secondary diamine **4d**. With aliphatic amines **1e** and **1f**, as well as with the aliphatic/aromatic **1g**, metathesis reactions were not accomplished (Scheme 3, Table S1). Several experiments in the presence of additives, such as Lewis acid Ti(O-*i*Pr)$_4$ [37], were also inconclusive. In a typical experiment, the substrate was recovered after column chromatography on SiO$_2$ (*e.g.* 50% for **1g**). Decomposition to unidentified compounds was also observed.

While amines are generally considered as poor substrates for ruthenium-based catalysts [19-23], some examples of successful olefin metathesis of unhindered tertiary amines have been disclosed [38-40]. We assume that in our case, similarly to related studies on interactions of ruthenium alkylidenes with amines [41-43], the basic nitrogen atoms in compounds **1e**, **1f**, and **1g** coordinate to the ruthenium intermediates (see Figure S2), resulting in species with low RCM activity.

Structure elucidation

The structure of **2a** (Figure 1a), **2b** (Figure 1b and Figure S3), and **3b** (Figure 1c) was confirmed by single-crystal X-ray diffraction analyses [44, 45]. Compounds **2a** and **2b** crystallize in space groups $P2_1/c$ and $P\bar{1}$, respectively. The former contains one molecule in the asymmetric unit, while the latter four. The ferrocenophanes are axially chiral owing to the shape of the bridge, however, the crystals contain their racemates. Both compounds crystallize with their aromatic substituents pointing away from the metathesis-derived macrocycle. Unfortunately, we were able to confirm only the connectivity of atoms in molecules **2b**. Single crystals of this compound diffracted X-rays weakly, and the obtained diffraction data are only significantly different from zero to ~1 Å which makes the derivation of any geometrical parameters of the structure impossible.

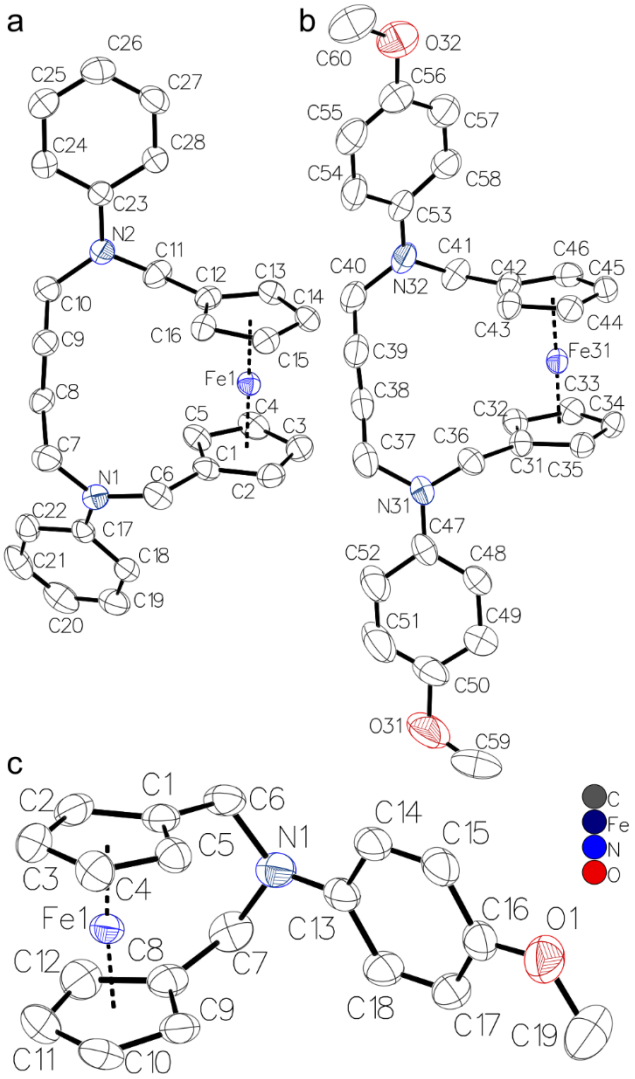

Figure 1: Molecular structure of compounds **2a** (a), **2b** (b) and **3b** (c). Thermal ellipsoids are shown at the 50% for **2a** and **3b**, and at the 30% probability level for **2b**. Hydrogen atoms are omitted for clarity. In the case of compound **2b** one molecule from the asymmetric unit is shown. For an overlay of all four molecules of **2b** from the asymmetric unit see Figure S3.

The two cyclopentadienyl rings are connected in a 1,2′ fashion by the 8-membered bridge containing two nitrogen atoms, two methylene groups, and the (*E*) isomer of a −CH=CH− group. The size of the macrocycle cavity in **2a**, defined as the distance

between the nitrogen atoms amounts to 5.340(4) Å. The calculated distance for **2b** (5.40 Å) is similar, see Figure S4.

While ferrocene moieties exhibit staggered conformation in **1a** and **1b** (Figures S5 and S6), they are forced toward an eclipsed conformation with the C1-Cg_a-Cg_b-C16 torsion angle equal to −13.0(2)° for **2a** (Cg_i denotes the cyclopentadienyl ring centroid). This angle equals 36° and 0° for staggered and eclipsed conformations, respectively. Similarly as in diamine **1a** (Figure S5), N1 and N2 atoms in ferrocenophane **2a** are almost coplanar with the adjacent carbon atoms, as their departure from the planes of these carbon atoms amounts to only 0.027(3) and 0.057(3) Å, respectively (Table S2). While the cyclopentadienyl planes are parallel in non-bridged compounds **1a** and **1b**, upon formation of the 8-membered bridges in **2a** and **2b**, the dihedral angle between the cyclopentadienyl rings increases slightly but does not exceed 1.0° (see Table S3 for details). The formation of a shorter 3-membered bridge in **3b** leads to a more significant inclination of the cyclopentadienyl planes with a dihedral angle of 9.61(12)° between them. This value is comparable to those reported for some related 2-aza-[3]ferrocenophanes [46-48].

Solution dynamics

The room temperature ^{1}H NMR spectra of **2a**-**2c** in $CDCl_3$ or toluene-d_8 reveal unresolved, doublet-like signals of allylic protons. Thus, the solution dynamics of **2b** was investigated in detail by variable temperature (VT) NMR in toluene-d_8 (Figure 2a) and CD_2Cl_2 (Figure 2b, Figure S7). Broadening of the bridging methylene (*b, b'*), cyclopentadienyl (*c*, *d*), and allylic (*e, e'*) resonances is clearly visible on lowering the temperature, while the appearance of the olefinic resonance (*a*) does not change considerably. The allylic doublet (*e*, *e'* at δ = 3.64 ppm at 25 °C) broadens at 0 °C,

disappears at −40 °C, and finally decoalescences at −80 °C into two broad signals (*e* and *e′*, δ = 4.04 and 2.98 ppm). Two cyclopentadienyl protons (*d and d′*) that resonate at δ = 3.76 ppm at 25 °C decoalescence at −80 °C into two broad signals (δ = 3.99 and 3.45 ppm) (Figure 2a, see also Figure S8 for the corresponding ^{1}H-^{13}C HSQC spectrum). We wish to note that these ^{1}H NMR spectra resemble those recorded for (*E*)-[6]ferrocenophanes in toluene-d_8 with four cyclopentadienyl and two allylic signals at low temperature [5].

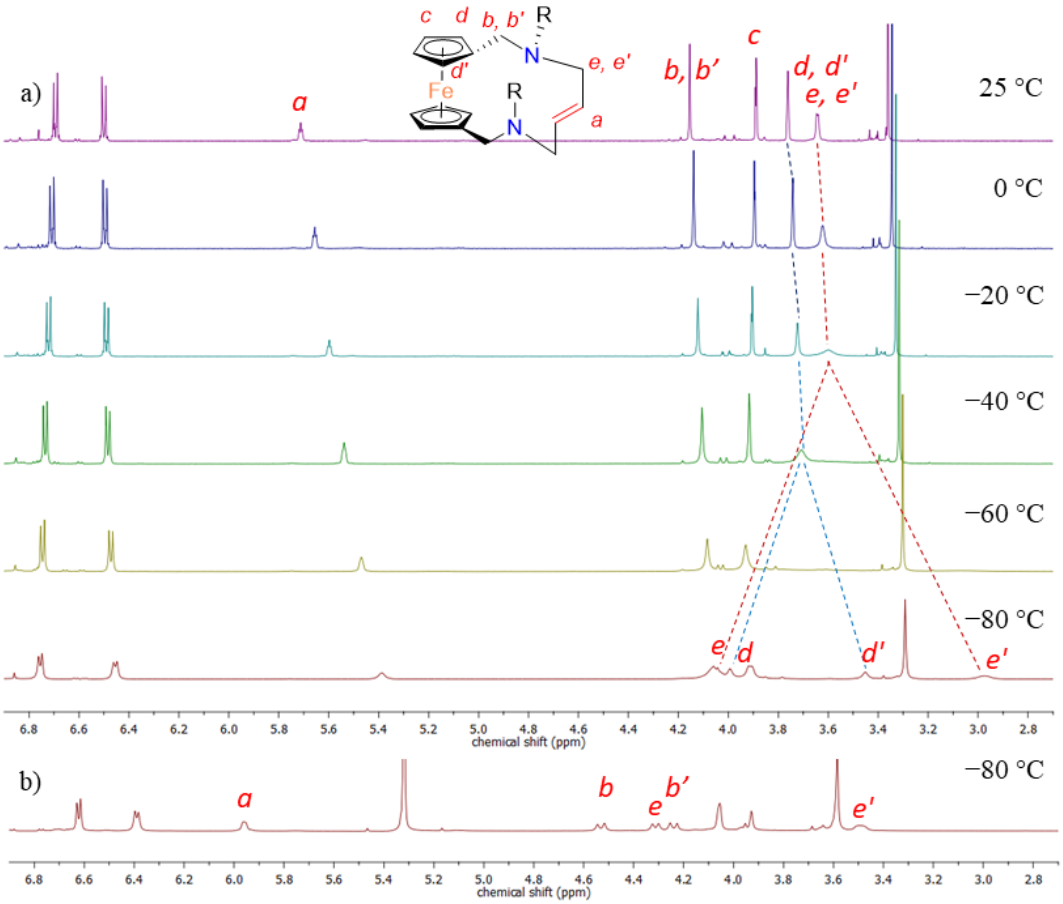

Figure 2: (a) The diagnostic range of VT ^{1}H NMR (600 MHz, toluene-d_8) spectra of **2b** (R = 4-MeO-C_6H_4). (b) The corresponding range of the ^{1}H NMR (600 MHz, CD_2Cl_2) spectrum of **2b** at −80 °C. VT ^{1}H NMR spectra of **2b** in CD_2Cl_2 from 25 °C to −93 °C are shown on Figure S7 in the Supporting Information.

Comparing the ^{1}H NMR spectra of **2b** recorded in toluene-d_8 (Figure 2a) and CD_2Cl_2 (Figure 2b and Figure S7), it is worth noting that the bridging methylene protons (*b* and *b'*, δ = 4.14 ppm at 25 °C) are not resolved into separate signals in toluene-d_8 down to −80 °C. However, in CD_2Cl_2 at −80 °C these protons are observed as two doublets (*b* and *b'*) at δ = 4.52 and 4.24 ppm ($^{2}J_{HH}$ = 16.8 Hz, Figure 2b). Moreover, the allylic protons (*e* and *e'*) are detected in CD_2Cl_2 as a doublet at δ = 4.31 ppm ($^{2}J_{HH}$ = 14.4 Hz) and a broad signal centred at δ = 3.49 ppm. The unequivocal assignment of these signals is based on the ^{1}H-^{13}C HSQC spectrum (Figure S8).

In order to identify the most likely process that could account for these solution phenomena, we have performed calculations on four conformers of **2b** with different orientations of the aromatic rings (Figures S9 and S10). The conformer with both aromatic rings located at the pseudoequatorial positions of the macrocycle (or pointing away from the macrocycle), that is analogous to the one observed in the solid state (Figures 1b and 3a), was found to be the most stable (Figure 3b). Compared to the most stable conformer, the predicted free Gibbs energy of a conformer with one aromatic substituent at the pseudoaxial position was higher by 13.1 kJ mol^{-1} at −80 °C and 9.9 kJ mol^{-1} at 25 °C (Table S5).

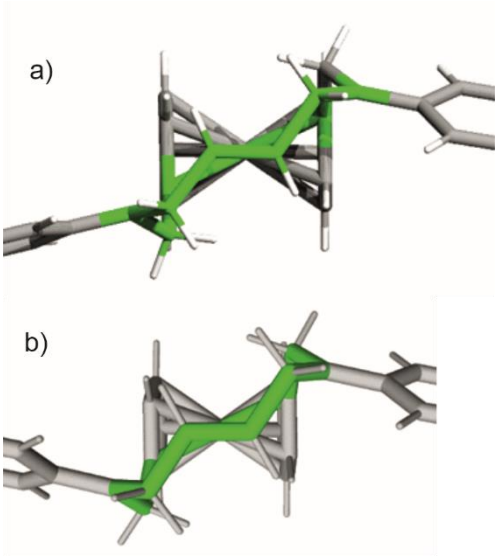

Figure 3: The 11-membered ring (highlighted in green) of compound **2b**: (a) according to the X-ray data; (b) calculated for the most stable conformer. The conformation of the ring could be considered analogous to the chair conformation of cyclohexane. The *N*-substituents (aromatic rings) are in pseudoequatorial positions.

The predicted ^{1}H NMR chemical shifts for all studied conformers (Figures S11-S15) correlate well with those observed experimentally at low temperature. For example, the difference between chemical shifts of the allylic protons $\Delta\delta$ = 1.06 ppm observed in toluene-d_8 at −80 °C is comparable to the calculated value $\Delta\delta$ = 1.1 ppm (on average). Therefore, we assume that the observed signals' inequivalences are due to the slow vibrations (on the NMR time scale) of the most stable conformer rather than to the presence of different conformers in the solution.

Conclusions

We have performed stereoselective, ruthenium-catalysed ring-closing metathesis (RCM) of α,ω-ferrocenyldienes **1**. These amino dienes have been obtained in a single step from 1,1′-ferrocenedicarboxaldehyde and *N*-allylanilines. Our synthetic approach

allows to obtain amine-containing substrates for RCM reactions bearing two different *N*-substituents. The resulting diaza[8]ferrocenophanes **2** are axially chiral in the solid state and reveal complex, solvent-dependent solution dynamics according to VT NMR studies. Their application as ligands for transition metals will be explored in our laboratory.

Experimental

Materials and methods

All metathesis reactions were performed under an argon atmosphere using Schlenk tube techniques. Dichloromethane was distilled from CaH_2. Toluene was distilled from Na/benzophenone, ethyl acetate was dried with MS 4Å. Further experimental details are provided in the Supporting Information.

Typical metathesis procedure

A solution of diamine **1a** (93.0 mg, 0.195 mmol) in CH_2Cl_2 (5.0 mL) was placed in a dry Schlenk flask. A solution of **GII** (7.0 mg, 0.0082 mmol, 4.2 mol%) in 5.0 mL of dry CH_2Cl_2 was added. The reaction mixture was stirred under reflux for 5 h on a water bath. Occasionally, the system was evacuated to remove the evolving ethene. The reaction mixture was left with stirring overnight at ambient temperature. A few drops of ethyl vinyl ether were added to the reaction mixture to deactivate the catalyst. The volatiles were removed on a vacuum pump. Dry toluene (2.0 mL) was added to the oily brown residue. The resulting suspension was then refrigerated at −70 °C overnight. The resulting precipitate was filtered off on a Celite® pad under argon. The filtrate was subjected to flash column chromatography (Al_2O_3 under argon, dry toluene:ethyl

acetate, 19:1, v/v). A yellow fraction was collected and evaporated to dryness on a rotary evaporator to yield yellow microcrystalline solid.

Compound 2a. Yield: 46.0 mg (0.103 mmol, 53%). mp: 195-200 °C (from CH_2Cl_2/*n*-hexane). ^{1}H NMR (500 MHz, $CDCl_3$) δ (ppm): 7.14–7.09 (m, 4H, C_6H_5), 6.62 (tt, J = 7.5, 1.0 Hz, 2H, C_6H_5), 6.58–6.55 (m, 4H, C_6H_5), 6.10–6.06 (m, 2H, =CH), 4.49 (s, 4H, C_5H_4-CH_2-N), 4.07 (app. t, J = 1.5 Hz, 4H, C_5H_4), 4.04 (b, 4H, N-CH_2-CH), 3.93 (app. t, J = 2.0 Hz, 4H, C_5H_4). ^{13}C{^{1}H} NMR (126 MHz, $CDCl_3$) δ (ppm): 147.72 (*ipso*-C_6H_5), 130.60 (=CH), 129.17 (C_6H_5), 116.31 (C_6H_5), 112.24 (C_6H_5), 88.28 (C_5H_4), 70.03 (C_5H_4), 66.49 (C_5H_4), 54.24 (N-*C*H_2-CH), 51.04 (N-*C*H_2-CH). HR MS (ESI) *m/z* found for $C_{28}H_{29}{}^{56}FeN_2$ $[M+H]^+$ 449.1668 (Calc. 449.1680). Anal. Calc. for $C_{28}H_{28}FeN_2$ × 0.4 H_2O: C 73.81, H 6.32, N 6.15; Found: C 74.15, H 6.39, N 6.42.

Compound 2b was obtained similarly from **1b** (64.9 mg, 0.121 mmol), **GII** (11.9 mg, 0.0140 mmol, 11 mol%) in CH_2Cl_2 (14.0 mL) and purified by column chromatography (Al_2O_3, dry toluene:ethyl acetate 19:1, v/v). Isolated as yellow needles from *n*-hexane. Yield: 31.5 mg (0.0620 mmol, 51%). mp: 102-106 °C (from CH_2Cl_2/*n*-hexane). ^{1}H NMR (500 MHz, $CDCl_3$) δ (ppm): 6.72 (d, J = 9.0 Hz, 4H, C_6H_4), 6.52 (d, J = 9.0 Hz, 4H, C_6H_4), 6.08-6.05 (m, 2H, =CH), 4.42 (s, 4H, C_5H_4-CH_2-N), 4.06 (app. t, J = 1.5 Hz, 4H, C_5H_4), 3.96 (b, 4H, N-CH_2-CH) overlapping with 3.94 (app. t, J = 1.5 Hz, 4H, C_5H_4), 3.70 (s, 6H, OCH_3). ^{13}C{^{1}H} NMR (126 MHz, $CDCl_3$) δ (ppm): 151.11 (*p*-C_6H_4), 142.70 (*ipso*-C_6H_4), 130.74 (=CH), 114.7 (C_6H_4), 113.30 (C_6H_4), 88.49 (C_5H_4), 69.87 (C_5H_4), 66.32 (C_5H_4), 55.73 (OCH_3), 54.56 (N-*C*H_2-CH), 50.85 (C_5H_4-*C*H_2-N). HR MS (ESI) *m/z* found for $C_{30}H_{33}{}^{56}FeN_2O_2$ $[M+H]^+$ 509.1893 (Calc. 509.1891). Anal. Calc. for $C_{30}H_{32}FeN_2O_2$ × 0.5 H_2O: C 69.63, H 6.57, N 5.41; Found: C 69.55, H 6.16, N 5.67.

From this fraction several orange crystals also crystallized that were collected and identified as **3b**. mp: 125-130 °C (from $CDCl_3$). ^{1}H NMR (500 MHz, $CDCl_3$) δ (ppm):

6.98 (dt, *J* = 9.5, 2.5 Hz, 2H, C_6H_4), 6.86 (dt, *J* = 9.0, 2.5 Hz, 2H, C_6H_4), 4.18 (app. t, *J* = 2.0 Hz, 4H, C_5H_4), 4.08 (app. t, *J* = 2.0 Hz, 4H, C_5H_4), 3.80 (s, 3H, OCH_3), 3.70 (s, 4H, CH_2). HR MS (ESI) *m/z* found for $C_{19}H_{20}{}^{56}FeNO$ $[M+H]^+$ 334.0901 (Calc. 334.0894).

Compound 2c was obtained from **1c** (60.1 mg, 0.119 mmol), **GII** (8.6 mg, 0.010 mmol, 8.4 mol%) in CH_2Cl_2 (18.0 mL) and purified by column chromatography (Al_2O_3, dry toluene:ethyl acetate, 19:1, v/v). Isolated as fine yellow needles from *n*-hexane. Yield: 29.8 mg (0.0623 mmol, 52%). mp: 120-124 °C (from CH_2Cl_2/*n*-hexane). ^{1}H NMR (500 MHz, $CDCl_3$) δ (ppm): 7.11 (t, *J* = 7.0 Hz, 2H, C_6H_5), 6.72 (d, *J* = 9.0 Hz, 2H, C_6H_4), 6.62 (dt, *J* = 7.0, 1.0 Hz, 1H, C_6H_5), 6.56 (d, *J* = 8.0 Hz, 2H, C_6H_5), 6.52 (d, *J* = 9.5 Hz, 2H, C_6H_4), 6.08-6.05 (m, 2H, =CH), 4.49 (s, 2H, C_5H_4-C*H*$_2$-N), 4.41 (s, 2H, C_5H_4-C*H*$_2$-N), 4.06 (app. q, *J* = 2.0 Hz, 4H, C_5H_4), 4.03 (b, 2H, N-C*H*$_2$-CH), 3.96 (b, 2H, N-C*H*$_2$-CH), 3.94 (app. t, *J* = 1.5 Hz, 2H, C_5H_4), 3.92 (app. t, *J* = 2.0 Hz, 2H, C_5H_4), 3.69 (s, 3H, OCH_3). ^{13}C{^{1}H} NMR (126 MHz, $CDCl_3$) δ (ppm): 150.27 (*p*-C_6H_4), 146.83 (*ipso*-C_6H_4 or C_6H_5), 141.78 (*ipso*-C_6H_4 or C_6H_5), 130.06 (=CH), 129.44 (=CH), 128.16 (C_6H_4 or C_6H_5), 115.34 (C_6H_4 or C_6H_5), 113.88 (C_6H_4 or C_6H_5), 112.38 (C_6H_4 or C_6H_5), 111.32 (C_6H_4 or C_6H_5), 87.68 (C_5H_4), 87.27 (C_5H_4), 69.11 (C_5H_4), 68.96 (C_5H_4), 65.49 (C_5H_4), 65.48 (C_5H_4), 54.90 (OCH_3), 53.60 (N-*C*H$_2$-CH), 53.36 (N-*C*H$_2$-CH), 50.19 (C_5H_4-*C*H$_2$-N), 49.90 (C_5H_4-*C*H$_2$-N). HR MS (ESI) *m/z* found for $C_{29}H_{31}{}^{56}FeN_2O$ $[M+H]^+$ 479.1785 (Calc. 479.1786). Anal. Calc. for $C_{29}H_{32}FeN_2O \times 0.5\ H_2O$: C 71.49, H 6.57, N 5.75; Found: C 71.43, H 5.92, N 5.84.

Similarly, compound **1d** (29.0 mg, 0.0514 mmol) and **GII** (3.0 mg, 6 mol%) were stirred and refluxed in CH_2Cl_2 (5.0 mL) for one week. A ^{1}H NMR spectrum indicated that **1d** was present in the reaction mixture, therefore GII (3.0 mg) was added and the stirring and heating was continued for an another week. Column chromatography (Al_2O_3, dry

toluene:ethyl acetate, 19:1, v/v) provided a yellow fraction (13.0 mg) that contained **1d**, **2d**, and other unidentified compounds. Compound **2d**: ^{1}H NMR (500 MHz, $CDCl_3$) δ (ppm): 6.14-6.10 (m, =CH). The second fraction was also collected and identified as compound **4d** (5.0 mg, yellow plates from CH_2Cl_2/*n*-hexane). ^{1}H NMR (500 MHz, $CDCl_3$) δ (ppm): 6.88 (dt, *J* = 7.5, 1.5 Hz, 2H, C_6H_4), 6.78 (d, *J* = 8.0 Hz, 2H, C_6H_4), 6.69-6.64 (m, 4H, C_6H_4), 4.62 (bs, 2H, NH), 4.34 (app. t, *J* = 1.5 Hz, 4H, C_5H_4), 4.24 (app. t, *J* = 2.0 Hz, 4H, C_5H_4), 4.08 (q, *J* = 7.0 Hz, 4H, O-C*H*$_2$CH$_3$), 3.95 (s, 4H, C_5H_4-*C*H_2), 1.45 (t, *J* = 7.0 Hz, 6H, O-CH$_2$C*H*$_3$). ^{13}C{^{1}H} NMR (126 MHz, $CDCl_3$) δ (ppm): 146.23 (C_6H_4), 138.47 (C_6H_4), 121.35 (C_6H_4), 116.71 (C_6H_4), 110.42 (C_6H_4), 110.22 (C_6H_4), 87.85 (C_5H_4), 68.58 (C_5H_4), 68.49 (C_5H_4), 63.83 (O-*C*H_2CH$_3$), 42.68 (C_5H_4-*C*H_2), 15.28 (O-CH$_2$*C*H$_3$). MS (EI) *m/z* (%), ^{56}Fe: 484 (M^+, 8), 347 (100), 270 (33), 241 (17), 240 (13), 163 (22). HR MS (EI) *m/z* found for $C_{28}H_{32}{}^{56}FeN_2O_2$ $[M]^+$ 484.1812 (Calc. 484.1813).

Supporting Information

Supporting Information File 1

Further experimental details, characterization of amino dienes **1**, amino aldehydes **S**, additional X-ray data, VT ^{1}H NMR spectra, 2D NMR spectra, and details of theoretical calculations.

Supporting Information File 2

X-ray data for ferrocenophane **2a**

Supporting Information File 3

X-ray data for ferrocenophane **2b**

Supporting Information File 4

X-ray data for ferrocenophane **3b**

Supporting Information File 5

X-ray data for diamine **1a**

Supporting Information File 6

X-ray data for diamine **1b**

Funding

This work was financially supported by National Science Centre (grant 2017/27/B/ST5/01495). Diffraction studies were supported by the Warsaw University of Technology.

References

1. Bauer, E. B.; Gladysz, J. A. Metal-Catalyzed Olefin Metathesis in Metal Coordination Spheres. In *Handbook of Metathesis*, *1st ed.*; Grubbs, R. H., Ed.; Wiley-VCH: Weinheim, Germany, 2003; Vol. 2, pp. 403–431.
2. Fiedler, T.; Gladysz, J. A. Multifold Ring-Closing Olefin Metatheses in Syntheses of Organometallic Molecules with Unusual Connectivities. In *Olefin Metathesis: Theory and Practice*; Grela, K., Ed.; John Wiley & Sons: 2014; pp. 311–328.
3. Locke, A. J.; Jones, C.; Richards, C. J. *J. Organomet. Chem.* **2001**, *637−639*, 669−676. doi: 10.1016/S0022-328X(01)00980-9
4. Ogasawara, M.; Nagano, T.; Hayashi, T. *J. Am. Chem. Soc.* **2002**, *124,* 9068−9069. doi: 10.1021/ja026401r
5. Buchowicz, W.; Guńka, P. A.; Buchalski, P.; Piszcz, M.; Buś, S.; Mrozowicz, M.; Mazur, M.; Wasilewski, R. *Organometallics* **2022**, *41*, 1968−1976. doi: 10.1021/acs.organomet.2c00163

6. Buchowicz, W.; Furmańczyk, A.; Zachara, J.; Majchrzak, M. *Dalton Trans*. **2012**, *41*, 9269−9271. doi: 10.1039/C2DT31291C

7. Ogasawara, M.; Wu, W. Y.; Arae, S.; Nakajima, K.; Takahashi, T. *Organometallics* **2013**, *32*, 6593−6598. doi: 10.1021/om400936b

8. Ogasawara, M.; Arae, S.; Watanabe, S.; Nakajima, K.; Takahashi, T. *Chem. Eur. J*. **2013**, *19*, 4151−4154. doi: 10.1002/chem.201300116

9. Hüerländer, D.; Kleigrewe, N.; Kehr, G.; Erker, G.; Fröhlich, R. *Eur. J. Inorg. Chem*. **2002**, 2633−2642. doi: 10.1002/1099-0682(200210)2002:10<2633::AID-EJIC2633>3.0.CO;2-4

10. Tumay, T. A.; Kehr, G.; Fröhlich, R.; Erker, G. *Dalton Trans*. **2009**, 8923−8928. doi: 10.1039/B911218A

11. Mazur, M.; Mrozowicz, M.; Buchowicz, W.; Koszytkowska-Stawińska, M.; Kamiński, R.; Ochal, Z.; Wińska, P.; Bretner, M. *Dalton Trans.* **2020**, *49*, 11504–11511. doi: 10.1039/D0DT01975E

12. Ogasawara, M.; Nagano, T.; Hayashi, T. *Organometallics* **2003**, *22*, 1174−1176. doi: 10.1021/om021058k

13. Ogasawara, M.; Watanabe, S.; Nakajima, K.; Takahashi, T. *Pure Appl. Chem.* **2008**, *80*, 1109−1113. doi: 10.1351/pac200880051109

14. Ogasawara, M.; Watanabe, S.; Nakajima, K.; Takahashi, T. *J. Am. Chem. Soc.* **2010**, *132*, 2136–2137. doi: doi.org/10.1021/ja910348z

15. Arae, S.; Nakajima, K.; Takahashi, T.; Ogasawara, M. *Organometallics* **2015**, *34*, 1197−1202. doi: 10.1021/om5011484

16. Sha, Y.; Zhang, Y.; Zhu, T.; Tan, S.; Cha, Y.; Craig, S. L.; Tang, C. *Macromolecules* **2018**, *51*, 9131−9139. doi: 10.1021/acs.macromol.8b02064

17. Otón, F.; Tarraga, A.; Espinosa, A.; Velasco, M. D.; Bautista, D.; Molina, P. *J. Org. Chem.* **2005**, *70*, 6603−6608. doi: 10.1021/jo050458p

18. Zhou, H.-Y.; Li, M.; Qu, J.; Jing, S.; Xu, H.; Zhao, J.-Z.; Zhang, J.; He, M.-F. *Organometallics* **2016**, *35*, 1866−1875. doi: 10.1021/acs.organomet.6b00237

19. Abramovitch, R. A.; Azogu, C. I.; Sutherland, R. G. *J. Chem. Soc. D* **1969**, 1439−1440. doi: 10.1039/C29690001439

20. Beer, P. D.; Chen, Z.; Drew, M. G. B.; Johnson, A. O. M.; Smith, D. K.; Spencer, P. *Inorg. Chim. Acta*, **1996**, *246*, 143−150. doi: 10.1016/0020-1693(96)05061-X

21. Tendero, M. J. L.; Benito, A.; Lloris, J. M.; Martínez-Máñez, R.; Soto, J.; Payá, J.; Edwards, A. J.; Raithby, P. R. *Inorg. Chim. Acta*, **1996**, *247*, 139−142. doi: 10.1016/0020-1693(95)04952-5

22. Khramov, D. M.; Rosen, E. I.; Lynch, V. M.; Bielawski, C. W. *Angew. Chem., Int. Ed*. **2008**, *47*, 2267−2270. doi: 10.1002/anie.200704978

23. Dey, S.; Wilson Quail, J.; Müller, J. *Organometallics* **2015**, *34*, 3039−3046. doi: 10.1021/acs.organomet.5b00340

24. Dey, S.; Sun, W.; Müller, J. *Inorg. Chem.* **2016**, *34*, 3630−3639. doi: 10.1021/acs.inorgchem.6b00170

25. Guthardt, R.; Blanckenberg, J.; Bruhn, C.; Siemeling, U. *Chem. Commun.* **2021**, *57*, 12984–12987. doi: 10.1039/D1CC05287J

26. Plenio, H.; Burth, D. *Organometallics* **1996**, *15*, 4054–4062. doi: 10.1021/om9602771

27. Mamane, V.; Fort, Y. *J. Org. Chem*. **2005**, *70*, 8220−8223. doi: 10.1021/jo0509758

28. Ogasawara, M.; Wada, S.; Isshiki, E.; Kamimura, T.; Yanagisawa, A.; Takahashi, T.; Yoshida, K. *Org. Lett.* **2015**, *17*, 2286−2289. doi: 10.1021/acs.orglett.5b01044

29. Sierra, M. A.; Rodríguez-Fernández, M.; Casarrubios, L.; Gómez-Gallego, M.; Allen, C. P.; Mancheňo, M. J. *Dalton Trans*. **2009**, 8399−8405. doi: 10.1039/B911450E

30. Hanson, P. R.; Maitra, S.; Chegondi, R.; Markley, J. L. General Ring-Closing Metathesis. In *Handbook of Metathesis*, *2nd ed*.; Grubbs, R. H.; O'Leary, D. J., Eds.; Wiley-VCH: Weinheim, Germany, 2015; Vol. 2, pp. 63−73.

31. Compain, P. *Adv. Synth. Catal*. **2007**, *349*, 1829−1846. doi: 10.1002/adsc.200700161

32. Wilson, G. O.; Porter, K. A.; Weissman, H.; White, S. R.; Sottos, N. R.; Moore, J. S. *Adv. Synth. Catal.* **2009**, *351*, 1817–1825. doi: 10.1002/adsc.200900134

33. Lummiss, J. A. M.; Ireland, B. J.; Sommers, J. M.; Fogg, D. E. *ChemCatChem* **2014**, *6*, 459–463. doi: 10.1002/cctc.201300861

34. Nascimento, D. L.; Reim, I.; Foscato, M.; Jensen, V. R.; Fogg, D. E. *ACS Catal*. **2020**, *10*, 11623−11633. doi: 10.1021/acscatal.0c02760

35. Mazur, M.; Ziemkiewicz, K.; Rawiak, K.; Kisiel, K.; Wińska, P.; Deresz, K.; Jarzembska, K. N.; Buchowicz, W. *Eur. J. Inorg. Chem*. **2022**, e202101098. doi: 10.1002/ejic.202101098

36. Alcaide, B.; Almendros, P.; Alonso, J. M. *Chem. Eur. J*. **2003**, *9*, 5793–5799. doi: 10.1002/chem.200305236

37. Yang, Q.; Xiao, W.-J.; Yu, Z. *Org. Lett.* **2005**, *7*, 871–874. doi: 10.1021/ol047356q

38. Ayad, T.; Genisson, Y.; Baltas, M.; Gorrichon, L. *Chem. Commun*. **2003**, 582−583. doi: 10.1039/B212217K

39. Badorrey, R.; Cativiela, C.; Díaz-de-Villegas, M. D.; Díez, R.; Gálvez, J. A. *Tetrahedron Lett*. **2004**, *45*, 719−722. doi: 10.1016/j.tetlet.2003.11.053

40. Kim, S.; Lee, J.; Lee, T.; Park, H.-G.; Kim, D. *Org. Lett.* **2003**, *5*, 2703–2706. doi: 10.1021/ol0349007

41. Occhipinti, G.; Bjørsvik, H.-R.; Törnroos, K. W.; Jensen, V. R. *Organometallics* **2007**, *26*, 5803–5814. doi: 10.1021/om070219n

42. Jong, H.; Patrick, B. O.; Fryzuk, M. D. *Organometallics* **2011**, *30*, 2333–2341. doi: 10.1021/om2000844

43. Rogalski, S.; Żak, P.; Tadeuszyk, N.; Pyta, K.; Przybylski, P.; Pietraszuk, C. *Dalton Trans*. **2017**, *46*, 1277−1282. doi: 10.1039/C6DT04290B

44. CCDC 2222236-2222238 and 2242035-2242036 contain the supplementary crystallographic data for this paper. All the data can be obtained free of charge from The Cambridge Crystallographic Data Centre via https://www.ccdc.cam.ac.uk/structures/. Raw diffraction data are available at https://doi.org/10.5281/zenodo.7330815.

45. Crystal Data for **1a**: $C_{30}H_{32}FeN_2$ (M = 476.42 g/mol): monoclinic, space group $P2_1/c$ (no. 14), a = 10.2946(2) Å, b = 10.13360(10) Å, c = 12.3564(3) Å, β = 104.866(2)°, V = 1245.89(4) Å^3, Z = 2, T = 293(2) K, μ(Mo Kα) = 0.625 mm^{-1}, 74020 reflections measured (6.82° ≤ 2Θ ≤ 65.7°), 4514 unique (R_{int} = 0.0359, R_{sigma} = 0.0149) which were used in all calculations. The final R_1 was 0.0401 ($I > 2\sigma(I)$), and wR_2 was 0.1072 (all data). Crystal Data for **1b**: $C_{32}H_{36}FeN_2O_2$ (M =536.48 g/mol): triclinic, space group $P\bar{1}$ (no. 2), a = 8.1888(2) Å, b = 9.2298(4) Å, c = 9.9792(5) Å, α = 74.069(4)°, β = 84.518(3)°, γ = 67.755(4)°, V = 671.26(5) Å^3, Z = 1, T = 293(2) K, μ(Mo Kα) = 0.594 mm^{-1}, 30443 reflections measured (6.43° ≤ 2Θ ≤ 66.0°), 4756 unique (R_{int} = 0.0540, R_{sigma} = 0.0428) which were used in all calculations. The final R_1 was 0.0471 ($I > 2\sigma(I)$), and wR_2 was 0.1226 (all data). Crystal Data for **2a**: $C_{28}H_{28}FeN_2$ (M = 448.37 g/mol): monoclinic, space group $P2_1/c$ (no. 14), a =

13.5944(8) Å, b = 9.3269(5) Å, c = 18.0996(10) Å, β = 107.951(7)°, V = 2183.2(2) Å^3, Z = 4, T = 293(2) K, μ(Mo Kα) = 0.709 mm^{-1}, 21873 reflections measured (6.4° ≤ 2Θ ≤ 57.2°), 5006 unique (R_{int} = 0.0418, R_{sigma} = 0.0390) which were used in all calculations. The final R_1 was 0.0488 ($I > 2\sigma(I)$), and wR_2 was 0.1323 (all data). Crystal Data for **2b**: $C_{30}H_{32}FeN_2O_2$ (M = 508.42 g/mol): triclinic, space group $P\bar{1}$ (no. 2), a = 9.0866(2) Å, b = 16.2580(3) Å, c = 36.9507(9) Å, α = 88.673(2)°, β = 87.895(2)°, γ = 81.185(2)°, V = 5389.8(2) Å^3, Z = 8, T = 293(2) K, μ(Mo Kα) = 0.588 mm^{-1}, 137542 reflections measured (4.85° ≤ 2Θ ≤ 55.0°), 24739 unique (R_{int} = 0.1072, R_{sigma} = 0.0921) which were used in all calculations. The final R_1 was 0.0624 ($I > 2\sigma(I)$), and wR_2 was 0.1846 (all data). Crystal Data for **3b**: $C_{19}H_{19}FeNO$ (M = 333.20 g/mol): orthorhombic, space group *Pbca* (no. 61), a = 19.3669(2) Å, b = 7.51090(10) Å, c = 20.7273(3) Å, V = 3015.05(7) Å^3, Z = 8, T = 293(2) K, μ(Mo Kα) = 1.00 mm^{-1}, 85694 reflections measured (6.87° ≤ 2Θ ≤ 65.7°), 5438 unique (R_{int} = 0.0372, R_{sigma} = 0.0156) which were used in all calculations. The final R_1 was 0.0341 ($I > 2\sigma(I)$), and wR_2 was 0.0897 (all data).

46. Sakano, T.; Ishii, H.; Yamaguchi, I.; Osakada, K.; Yamamoto, T. *Inorg. Chim. Acta* **1999**, *296*, 176–182. doi: 10.1016/S0020-1693(99)00369-2
47. Chen, L.; Cui, X.; Cheng, H.; Chen, X.; Song, M.; Tang, M.; Wei, D.; Wu, Y. *Appl. Organomet. Chem.* **2012**, *26*, 449–454. doi: 10.1002/aoc.2839
48. Dwadnia, N.; Allouch, F.; Pirio, N.; Roger, J.; Cattey, H.; Fournier, S.; Penouilh, M.-J.; Devillers, C. H.; Lucas, D.; Naoufal, D.; Ben Salem, R.; Hierso, J.-C. *Organometallics* **2013**, *32*, 5784–5797. doi: 10.1021/om400317s